Reversible Watermarking for Knowledge Digest Embedding and Reliability Control in Medical Images

Gouenou Coatrieux, *Member, IEEE*, Clara Le Guillou, Jean-Michel Cauvin, and Christian Roux, *Fellow, IEEE*

***Abstract*—To improve medical image sharing in applications such as e-learning or remote diagnosis aid, we propose to make the image more usable by watermarking it with a digest of its associated knowledge. The aim of such a knowledge digest (KD) is for it to be used for retrieving similar images with either the same findings or differential diagnoses. It summarizes the symbolic descriptions of the image, the symbolic descriptions of the findings semiology, and the similarity rules that contribute to balancing the importance of previous descriptors when comparing images. Instead of modifying the image file format by adding some extra header information, watermarking is used to embed the KD in the pixel gray-level values of the corresponding images. When shared through open networks, watermarking also helps to convey reliability proofs (integrity and authenticity) of an image and its KD. The interest of these new image functionalities is illustrated in the updating of the distributed users' databases within the framework of an e-learning application demonstrator of endoscopic semiology.**

***Index Terms*—Medical image security, medical image sharing, medical knowledge management, reversible watermarking.**

I. Introduction

MEDICAL image sharing is used in a wide variety of applications ranging from telediagnosis to telesurgery, and it also promotes applications such as remote diagnosis aid and e-learning. These two latter applications are made possible by the ability to compare images to previously diagnosed examinations [1]. Beyond image comparison, similarity search between examinations requires medical knowledge representation.

Inspired by medical practice, we have defined a bilevel–diagnosis and findings—description language in endoscopy in order to unify the representation of diseases and cases. Based on this analysis of the diagnostic reasoning process, we derived a decision aid system: an *advanced endoscopic atlas* [2], [3], which exploits the image semantic content to suggest consistent diagnostic hypotheses illustrated by cases relevant to the problematic case description. This system relies on two bases. The first one defines endoscopic knowledge and the second one corresponds to the base of cases—images with their symbolic description. The relevant case retrieval first consists of a classification process based on endoscopic knowledge in order to identify potential cases within the same class as the problematic case. Cases that belong to the eligible diagnostic classes are then selected and sorted according to their similarity with the problematic case. This system, resulting from a previous work [3], is at the midpoint between pattern recognition [4] and case base reasoning paradigms [5].

This knowledge base, and in particular the finding level, represents the first attempt to define an endoscopic finding semiology. In this paper, our concern is to promote and spread this expertise. The basic principle of our approach is to share a medical image with a knowledge digest (KD). The proposed KD gives a synthetic medical description and interpretation of the image content. In the framework of an e-learning application demonstrator project, this digest will constitute the distributed knowledge and will thereafter be exploited in order to: 1) update the user's case and knowledge bases and 2) provide the means for similar image retrieval with either the same findings or differential diagnoses.

To share medical images with some concomitant data, one approach involves adding, when allowed by the image file format, some extra header information. Unfortunately, header files are prone to manipulation and information loss may occur during file format conversion. For example, most data contained in the header of a Digital Imaging and Communications in Medicine (DICOM) [6] image file will be lost after conversion into another multimedia format like Joint Photographic Experts Group (JPEG).

In our scheme, we have opted for watermarking to share data [7]. When watermarking is applied to images, it allows the insertion of a message by modifying the pixel gray-level values of the image in an imperceptible manner. The embedded information is attached to the signal itself, independently of the image file format, introducing information management and protection levels as near as possible to the data [8]. It is usually required that the watermarked information remains hidden from any unauthorized user (as with data encryption, a secret key is needed to access the watermark content). In addition,

Manuscript received April 30, 2007. First published October 31, 2008; current version published March 3, 2009. This work was supported by the Regional Center for Innovation and Technology Transfer (CRITT) Santé Bretagne and the Regional Council of Brittany under Project SPROGIMMAD.

G. Coatrieux and C. Roux are with the Institut Télécom, Télécom Bretagne, Brest CS 83818-29238, France, and also with the Institut National de la Santé et de Recherche Médicale (INSERM) U650, Brest 29609, France (e-mail: gouenou.coatrieux@telecom-bretagne.eu; christian.roux@telecom-bretagne.eu).

C. Le Guillou and J-.M. Cauvin are with the University Hospital of Brest, Brest 29609, France, and also with the Institut National de la Santé et de Recherche Médicale (INSERM) U650, Brest 29609, France (e-mail: clara.leguillou@chu-brest.fr; jean-michel.cauvin@chu-brest.fr).

Color versions of one or more of the figures in this paper are available online at http://ieeexplore.ieee.org.

Digital Object Identifier 10.1109/TITB.2008.2007199

distortions due to the watermarking should not interfere with the use of the watermarked object. For medical images, the image interpretation should not be altered. Among the different approaches proposed for watermarking medical images [8], we have retained lossless or reversible watermarking. The reversibility property allows the removal of the watermark from the image and the exact retrieval of the original image.

In the present e-learning application, lossy compressed endoscopic images are shared. If there is no impediment to using a slight lossy compression, since it does not impair the physician's interpretation [9], reversible watermarking has attractive properties in terms of not further compromising image interpretation. For that purpose, we extend an improved version of the reversible watermarking method we proposed in [10] for raw images to JPEG-compressed images.

Hence, suggested KD and watermarking are jointly exploited at the database level of our demonstrator. At the same time, since such information is used to update databases through open networks like the Internet, it should be possible to verify the reliability of the image and its KD. Hence, the message that is watermarked also provides data integrity and authenticity control as it contains a digital signature computed on both the image and its KD, along with the date of creation and an authenticity code (i.e., proof of data origins).

To our knowledge, this paper is the first that proposes to embed metadata that are not an element of the electronic patient record (EPR) or data for protecting the image.

The rest of this paper is organized as follows. In Section II, medical knowledge representation and the proposed KD definition are discussed. In Section III, our reversible watermarking scheme and its adaptation to JPEG-compressed images are presented. Section IV is devoted to the constitution of the KD watermark and the architecture of the e-learning demonstrator for endoscopic semiology. Concluding remarks are given in Section V.

II. Medical Image Knowledge in Digestive Endoscopy

Before presenting the KD structure, we summarize the key points about information representation and reasoning in digestive endoscopy, a representation we have considered in our *advanced endoscopic atlas* and on which the KD relies.

A. Endoscopic Information and Reasoning

1) Information Representation: Mechanisms that allow endoscopists to go from observation to endoscopical findings and from endoscopical findings to endoscopical diagnosis make use of their varied knowledge, including that acquired by training and experience: anatomic knowledge of the normal and surgically modified digestive cavity, knowledge of elementary descriptors of endoscopical findings, and knowledge of the combination of endoscopical findings and the medical context.

In this framework, we have developed a bilevel description language of endoscopic imaging and of gastroenterology diseases. This language is partly based on the minimal standard terminology of the European Society of Gastroenterology [11] and handles the symbolic content of images with respect to endoscopy imaging. For further details, the reader may refer to [3]. However, this language exemplifies the concept of *Scenes* with *Objects*.

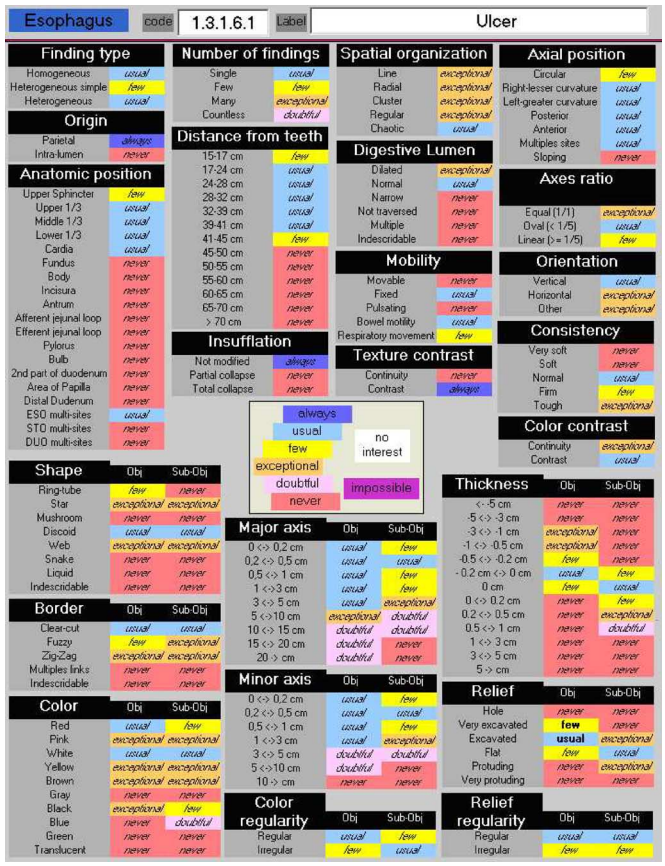

Fig. 1. Example of a finding object. Finding features are in black boxes and just below in gray their possible "attributes" (i.e., values). Color variations indicate the linguistic valuation (LV) of the attributes.

1) The Scene represents the disease level. It is an endoscopic diagnosis that associates one patient context with one or several endoscopic finding(s) and their spatial relations.
2) The Object represents the finding level. It is a finding diagnosis in a scene and is described through different features.

Here, the symbolic description of one finding rests on 33 features. One feature can take different values that we call *attributes*. For example, in Fig. 1, the feature "color regularity" can be described as "regular" or "irregular." Based on clinical expertise, 206 attributes are currently considered [3].

2) Knowledge and Case Bases: This representation of the endoscopic information and this language have resulted in the creation of a knowledge base and a case base.

The knowledge base gives an *a priori* description of 150 scenes (diseases) and 100 objects (endoscopic findings). For one object or finding in this base, an LV is assigned to each of its attributes. With LV values, the expert expresses his knowledge while instilling uncertainty or vagueness [12]. More precisely, an object feature can be judged as: 1) *without interest*, then all its attributes too; 2) *impossible*, then all its attributes too; and 3) *of interest*, then each attribute is denoted as *never*, *exceptional*,

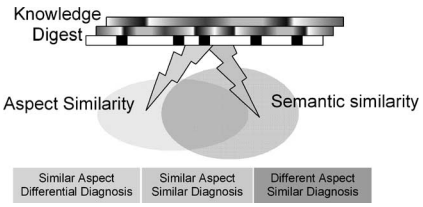

Fig. 2. Knowledge digest.

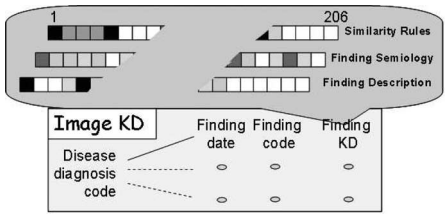

Fig. 3. Knowledge digest structure.

rare, *frequent*, *always*, or at least *doubtful* when the choice between *never* and *exceptional* cannot be stated. An example of such a finding description is given in Fig. 1. It can be seen that a finding is identified with a code and a label. We also retrieve the 33 features and their corresponding attributes with assigned LV values.

Scenes are described in a similar way in this base. They are depicted by the objects, the possible spatial relations between these objects, and by a patient profile (gender and age prevalence features as well as a predefined set of clinical contexts).

The case base is constituted of indexed images, each representing an endoscopic diagnosis with one or more findings. In this base, one finding is described using the 206 attributes: *the finding description*. As one image illustrates a particular realization of one finding, there is no uncertainty in the valuation of the attributes. Consequently, each attribute is set to *true* or *false* if it describes the finding.

3) Reasoning With Knowledge and Cases: For a new situation, the similar case retrieval starts by identifying potential findings, based on the knowledge base and the description of the problematic case. Then, disease classes are identified through all possible combinations of identified findings. The next step reevaluates the ranking of potential findings in the context of potential diseases. Then, the classification process is carried out.

The retrieval process is completed by searching among these potential classes of diseases and findings, the most similar cases in the case base. For this task, the description of the problematic case is compared, feature to feature, with case descriptions in the case base. This comparison makes use of *similarity rules* that express the relationships between the different attributes of the same feature. Two attributes of the same feature are judged as *incompatible*, *not similar*, *slightly similar*, *fairly similar*, or *identical*. The rules are represented by double entry tables. There are at least 33 of these tables.

At the end of this retrieval, potential findings and diseases similar to the problematic case are illustrated with case examples.

B. Knowledge Digest (KD)

In this context and in the spirit of case base reasoning (see Fig. 2), one KD is associated to one image, considering that it must be sufficient to retrieve similar images with either the same findings or differential diagnoses. For that purpose, one KD synthesizes the symbolic descriptions of one image, those of the findings semiology as the similarity rules.

As illustrated in Fig. 3, the KD structure is composed of a diagnosis code, and for each identified finding, a date, a code, and its related finding KD. The "finding date" will be used in the updating routines of the demonstrator knowledge (see Section III).

The finding KD is represented by three vectors: the finding description vector, the finding semiology vector, and the similarity rules vector. Each of these has 206 components, and one component is associated with one attribute (see Section II-A2). The finding description vector is a binary vector whose components are set to "1" if the corresponding attributes describe the finding or to "0" on the contrary. The finding semiology vector translates the knowledge we have about the finding. Each of its components takes its value between 0 and 5 representing the LV valuation from "*never*" to "*always*" (see Section II-A2). The third vector corresponds to the similarity rules described in Section II-A3. Each value, from "*incompatible*" to "*identical,*" is associated with a numerical value 0, 1, 2, 3, or 4.

Like the image, the KD with its synthetic representation of endoscopic information is language-independent, unlike the glossary that allows its interpretation. We propose to share such a KD with its associated image. The KD is a tool from which dynamic learning scenarios can be elaborated so as to surf between similar images with either the same or differential diagnoses.

III. Enhancing Image Functionalities With Watermarking

Watermarking integrates metadata and/or protection data in an image by modifying its pixel gray-level values. It provides an original way to share related data, like an image and its KD.

The method we use is lossless or reversible. This means that the watermark can be suppressed from the image. The method we summarize shortly is an improved version of that described in [10] and [13]. This method is now parameter-free and adapted in this paper to lossy JPEG-compressed images.

A. Reversible Watermarking Scheme

Our scheme is additive; it derives from the message to be embedded a watermark signal that is added to the image I. This digital signal consists of a matrix constituted of negative or positive integer values. Because of the limited image depth ($2^p - 1$ possible gray levels for a p-bit depth image), the watermark signal, once added to the image, can introduce underflows and overflows [14], i.e., pixels with a gray value outside the range $[0, \ldots, 2^p - 1]$. For example, within an image of 8-bit depth, subtracting one gray level from a pixel of gray value 0 will give a negative value that cannot be encoded: it is an underflow. Hence, not all of the image pixels can be watermarked.

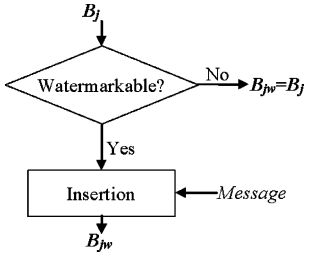

Fig. 4. Reversibility principle of our method: a classifier decides if one block B_j can be watermarked without introducing an underflow or an overflow.

As depicted in Fig. 4, to prevent underflows and overflows, our scheme makes use of a pixel block classification to distinguish watermarkable and nonwatermarkable blocks in the image. Nonwatermarkable blocks are those that will introduce an overflow or an underflow if they are watermarked. Hence, nonwatermarkable blocks will not be modified, while the insertion process will proceed with embedding the message in the watermarkable blocks. At the detection stage, to ensure retrieval of the watermarked blocks from the watermarked image I_w, this classification is built on an image estimation invariant to the insertion process. Unless the watermarked image is modified, the watermarked reader will retrieve the classifier easily.

For this experiment, our method works in the following way. Image I is separated into 2×2 pixels blocks $\{B_j\}$. If one block $B_j = [x_{0j}, x_{1j}, x_{2j}, x_{3j}]$ is watermarkable, it will be modified to B_{jw} by adding or subtracting a known watermark pattern W, herein defined as:

$$W = \begin{bmatrix} \delta_0 & \delta_1 \\ \delta_2 & \delta_3 \end{bmatrix} = \begin{bmatrix} 1 & -1 \\ -1 & 1 \end{bmatrix}. \tag{1}$$

For the classification process, each pixel of a block B_j is estimated though a linear combination of all the pixels of B_j leading to $\hat{B}_j = [\hat{x}_{0j}, \hat{x}_{1j}, \hat{x}_{2j}, \hat{x}_{3j}]$, where:

$$\begin{aligned} \hat{x}_{0j} &= \frac{[2x_{0j} + x_{1j} + x_{2j}]}{4} \\ \hat{x}_{1j} &= \frac{[2x_{1j} + x_{0j} + x_{3j}]}{4} \\ \hat{x}_{2j} &= \frac{[2x_{2j} + x_{0j} + x_{3j}]}{4} \\ \hat{x}_{3j} &= \frac{[2x_{3j} + x_{1j} + x_{2j}]}{4}. \end{aligned} \tag{2}$$

As stated earlier, $\hat{B}_j$ remains unchanged if W is added to or subtracted from B_j (i.e., $\hat{B}_j = \hat{B}_{jw}$).

The classification process involved aims at differentiating blocks for which the addition (or subtraction) of W leads to an overflow or an underflow from the others. Each block B_j will be classified depending on two values $(\hat{B}^j_{\min}, \hat{B}^j_{\max})$ derived from $\hat{B}_j$ and used to avoid underflow and overflow, respectively:

$$\begin{aligned} \hat{B}^j_{\min} &= \min_{i=0,\ldots,3} \{\hat{x}_{ij}, \hat{x}_{ij} \in \hat{B}_j\} \\ \hat{B}^j_{\max} &= \max_{i=0,\ldots,3} \{\hat{x}_{ij}, \hat{x}_{ij} \in \hat{B}_j\}. \end{aligned} \tag{3}$$

From this block characterization, the classifier consists of two thresholds $(T_{\min}, T_{\max})$ computed on the N_u blocks at the origin of an underflow and the N_o blocks at the origin of an overflow:

$$\begin{aligned} T_{\min} &= \max_{i=0,\ldots,N_u} \{\hat{B}^i_{\min}\} \\ T_{\max} &= \min_{i=0,\ldots,N_o} \{\hat{B}^i_{\max}\}. \end{aligned} \tag{4}$$

Consequently, the watermarkable blocks are those whose characteristics satisfy $\hat{B}^j_{\min} > T_{\min}$ and $\hat{B}^j_{\max} < T_{\max}$.

At the detection stage, the watermark reader applies the same procedure in order to retrieve the classifier. However, in a few cases, the thresholds are changed after the insertion process making the message retrieval impossible. To overcome this issue, our scheme embeds the message in two steps. First, the embedder considers the thresholds that the watermark reader will identify and inserts the original values $T_{\min}, T_{\max}$ and one part of the message in the corresponding blocks. The rest of the message is then embedded by modifying the last watermarkable blocks.

Once the watermarkable block set is identified, a binary message M is inserted according to the following procedure.

1) Watermarkable blocks are ordered secretly depending on a user's secret watermarking key.
2) For one block B_k, one pixel x_{0k} is selected and compared to its estimate $\hat{x}_{0k}$:
   a) If $\|x_{0k} - \hat{x}_{0k}\| < 1$, then B_k is able to convey 1 bit b of M. B_k is called a *carrier block* and is modified in the following manner:

$$\begin{aligned} &\text{if } b = 1, \quad \text{then } B_{kw} = B_k + W \implies x_{0kw} > \hat{x}_{0k} \\ &\text{if } b = 0, \quad \text{then } B_{kw} = B_k - W \implies x_{0kw} < \hat{x}_{0k}. \end{aligned} \tag{5}$$

   At the detection stage, the watermark reader has to interpret only the relationship between x_{0k} and $\hat{x}_{0k}$ to decode the message and restore B_k.
   b) If $\|x_{0k} - \hat{x}_{0k}\| \geq 1$, then B_k is called a *noncarrier block* as the relationship between x_{0k} and $\hat{x}_{0k}$ cannot be modified. For such a block, the distance between x_{0k} and $\hat{x}_{0k}$ is increased by adding or subtracting W.

At detection, once the classifier is rebuilt and the watermarkable blocks are retrieved and reordered, the watermark reader restores the blocks by adding or subtracting the pattern W depending on the relationship between x_{0kw} and $\hat{x}_{0k}$. These relationships also help to reidentify carrier blocks, and consequently, read the watermarked message.

This method is parameter-free and minimizes image distortion. However, message and exact image recovery are possible only if the watermarked image has not been modified, since the watermark is fragile.

B. Extension to JPEG-Compressed Images

JPEG [15] is a popular and well-known standard for image compression that allows two compression modes, namely, lossless and lossy. The first reduces only the image file size through

an entropic encoding, while the second, which we consider hereafter, authorizes some information loss according to an integer quality factor $\delta \in [0, \ldots, 100]$. As δ decreases, the compression file size ratio increases and the image quality is less well preserved.

As mentioned earlier, the previous watermarking method is fragile. Message extraction and watermark removal will not be possible after the image has been altered. Consequently, this method cannot be applied before lossy compression but after the information loss has occurred. Hence, embedding will be performed in the information preserved after compression. For JPEG, this information is located in the frequency domain.

For color images, the JPEG algorithm starts by an image color transformation into the YUV space. For each block of 4 pixels, there are four samples of luminance information (Y) and one sample of each of the two chrominance components (U and V). Each color component is treated independently. The process continues by splitting the image (or one color component) into 8×8 pixel blocks. A discrete-cosine transform (DCT) is then applied to each block, leading to blocks of 8×8 transformed coefficients C_{nm}:

$$C_{nm} = \sum_{i=0}^{7} \sum_{j=0}^{7} \Phi(i,j) \alpha_i \alpha_j B_{ij} \tag{6}$$

where B_{ij} corresponds to one pixel of the block with:

$$n = 0, \ldots, 7 \qquad m = 0, \ldots, 7$$

$$\Phi(i,j) = \cos\left(\frac{\pi(2i+1)j}{16}\right) \cos\left(\frac{\pi(2j+1)}{16}\right)$$

$$\alpha_i = \sqrt{\frac{2}{16}}, \qquad i \neq 0; \qquad \alpha_0 = \sqrt{\frac{1}{16}}.$$

One coefficient C_{nm} is associated with a spatial frequency (n, m). C_{00}, also called the dc coefficient, is proportional to the mean gray-level value of the block. The remaining of the coefficients (AC coefficients) take their value in the range $[-1024, \ldots, 1023]$. This has its importance because it limits the signal dynamics. Hence, embedding in the frequency domain is also subject to overflow and underflow.

In the compression process, information loss is achieved by applying a uniform quantization to each coefficient. The quantization step varies from one coefficient to another and is derived from a standard quantization table Q modulated by the quality factor δ. Once the quantization process is done, entropic encoding is applied to quantized DCT coefficients in order to constitute the JPEG bitstream. Hence, to reversibly watermark JPEG images, our method will be applied after the information loss, i.e., on the integer values C^q_{nm} that are the quantized DCT coefficients:

$$C^q_{nm} = \lfloor C_{nm} / Q_\delta(n,m) \rfloor. \tag{7}$$

The adopted strategy embeds parts of the message independently in several coefficient planes. A coefficient plane P_{nm} groups all the image coefficients of the same spatial frequency (n, m), with coefficient values varying in the range: $[\lfloor -1024/Q_\delta(n,m) \rfloor, \ldots, \lfloor 1023/Q_\delta(n,m) \rfloor]$. Hence, our watermarking algorithm remains the same for one-coefficient plane; only the thresholds $T_{\min}$ and $T_{\max}$ that control underflows and overflows have to be refined according to this interval. Note that each time the image is recompressed with a different quality factor the watermark signal will have to be recomputed.

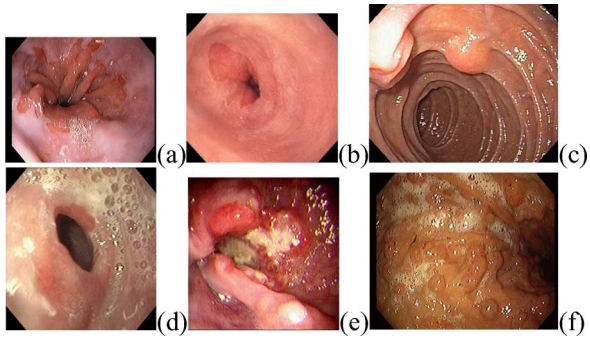

Fig. 5. Illustrative examples. (a) Barrett esophagus. (b) Esophagitis. (c) Nodules. (d) Stenosis. (e) Tumor. (f) Polyps.

Depending on the message length, the number of watermarked coefficient planes may vary in order to reach the requirement in terms of capacity (i.e., the number of bits to be embedded within one image). As a consequence, the watermark may become more or less visible depending on the number of coefficient planes used for embedding. Hence, the performance of the method depends on the size of the message, the dimensions, and the content of the image. The KD structure takes this into account.

IV. Endoscopic Semiology E-Learning Application

The proposed KD and watermarking abilities have been jointly experimented at the database level of an e-learning demonstrator for endoscopic semiology. This system shares lossy compressed endoscopic images that give illustrative examples of eight distinct diseases (see Fig. 5): Barrett esophagus, esophagitis, nodules, stenosis, tumor, polyps, ulcer, and varices.

Currently, the system makes use of JPEG compression. Some studies have been conducted with endoscopic images to evaluate the ratios of compression that are acceptable in order to reduce the data volume while maintaining quality for clinical review. It has been shown in [16] that no subjects could tell the difference between original noncompressed images and 1:10 lossy JPEG-compressed images.

In this application, knowledge digests are shared with images through fragile watermarking. This may not be common as fragility is a property usually required for image integrity verification. For metadata watermarking, the need for robust insertion in opposition to fragile insertion depends on the application framework. In our medical context, the KD may no longer be representative of the image if the latter is modified. Consequently, fragile watermarking is acceptable in this case.

In the next section, we present and discuss KD embedding, and thereafter we introduce the system architecture and some scenarios of use.

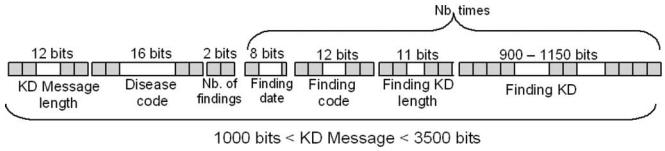

Fig. 6. KD message organization.

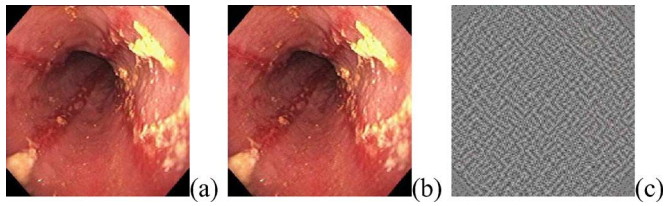

Fig. 7. Example of an image watermarked with its KD. (a) Original image of 365×378 pixels. (b) Watermarked image—set of coefficient planes considered $\zeta = \{P_{nm}/n = 0, \ldots, 2; m = 0, \ldots, 2; (n, m) \neq (0, 0)\}$. Capacity = 2373 bits. PSNR = 41.7 dB. (c) Image of difference: the watermark.

A. Watermarking Endoscopic Image Knowledge

The KD associated with a single image will in fact be converted to the smallest possible binary string before its insertion. The smaller the KD, the less visible the watermark (see Section III). As shown in Fig. 6, the KD to be watermarked contains the total message length, the diagnosis code, the number of identified findings, and, for each finding, the finding's code and length followed by the finding KD itself. In order to minimize the size of the whole message to be embedded, the three finding KD vectors (see Section II-B) are compressed before being binarized.

In general, images display one or two lesions, exceptionally three. Thus, the average size of the image KD is between 1000 and 2000 bit, reaching a maximum of 3500 bit.

In our experiments, a test set of 750 images was considered. We first decided to apply the insertion process only to the Y component of JPEG-compressed images. However, the proposed scheme can easily be extended to the three color components.

As described in Section III-B, our algorithm adaptively chooses a set of coefficient planes $\{P_{nm}\}$ to reach the capacity requirement for message embedding. The capacity depends on the number of coefficient planes retained and also on the image size and content. Over the whole image test set, the smallest, average, and maximum capacities, expressed in bits of message per image pixel (bpp), considering the set of coefficient planes $\zeta = \{P_{nm}/n = 0, \ldots, 3; m = 0, \ldots, 3; (n, m) \neq (0, 0)\}$, are, respectively, 0.028, 0.046, and 0.0552 bpp. For an image of 368×368 pixels, the smallest message we may expect to embed is around 3700 bit.

The reversibility of our method guarantees that once the watermark is removed, the image distortion observed is only due to the compression information loss. However, keeping the watermark in the image leads to more distortion. Here, we make use of the peak SNR (PSNR) in order to quantify the distortion between the original JPEG image I and its watermarked version I_W:

$$\text{PSNR}(I, I_W) = 10 \text{ Log}_{10} \left(\frac{NM(2^p - 1)^2}{\sum_{n,m=1,1}^{N,M} (I_{nm} - I_{W\,nm})^2} \right) \tag{8}$$

where p, N, and M correspond to the image depth and dimensions, respectively.

Considering the same experiment as previously, we have found the smallest, average, and maximum distortion to be (considering the image Y component) 37.4, 37.68, and 39.67 dB, respectively. However, in practice, capacity requirements are satisfied for images of dimensions 480×640 pixels with a PSNR of 42.36 dB; only three coefficient planes are used. The watermarked images were evaluated by one physician involved in the project. He did not perceive the distortions due to the watermark. Hence, we may consider that such distortion results are considered as acceptable in an e-learning framework. In Fig. 7, we give an example of an image watermarked with its KD.

Nevertheless, an additional study needs to be conducted in order to evaluate the possible risks of interference between the watermark and the image interpretation. This study will combine physicians' evaluations with other objective measures of perceptual quality like the normalized rms error (NMRSE) in order to determine the best parameters of the method. In any case, the method is lossless and allows us to retrieve the original compressed image after suppressing the watermark distortion. This supports the idea that our approach can be used in the framework of remote diagnosis aid applications.

B. Illustrative use in an E-Learning Demonstrator System

Our demonstrator, under development, is implemented using Matlab (MathWorks) and an Apache Web Server. It will be an extension of the Web atlas site (http://i3Se009d.univ-brest.fr/) [3]. As depicted in Fig. 8, its architecture is based on a Web server that gives access to an image database through a Web site publicly available. A user has to access only the appropriate URL. With Matlab installed on his/her computer, the user will be able to benefit from the distributed functionalities.

As depicted in Fig. 8, before images are made available on the Web site, each image is lossy compressed with JPEG at a predefined factor of quality. At the same time, the image KD is constituted from the different databases. Both the image and the KD are the inputs of the "reliability protection and watermarking" box whose content is described in Fig. 9.

Reliability is maintained through one digital signature (DS) computed on the image, the KD, the date of creation, and the Web server authenticity code. This signature will be used by the user system to verify the reliability of the information, i.e., verifying integrity and origin of this dataset. In fact, any difference between this signature and the recomputed one will indicate that data have been corrupted. In our experiment, we use the digital signature algorithm (DSA) signature [17] that provides a 160-bit-long DS. This signature produced with the Web server private key K_{pr} (this key is only known to the Web server) can only be verified by making use of the public key K_{pu} of the

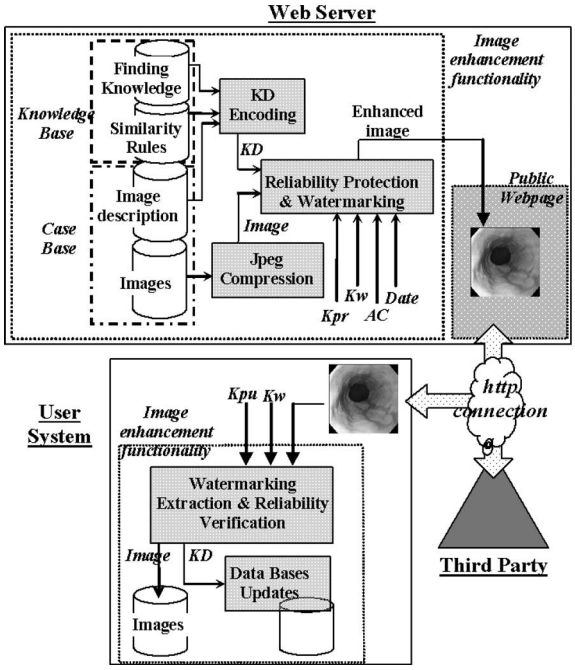

Fig. 8. System architecture. Before being made available on a public Web page, one image is watermarked with its KD. Kpr, Kpu, Kw, AC, and date correspond to the private and public keys of the Web server, the watermarking secret key, the Web server authenticity code, and the KD creation date, respectively.

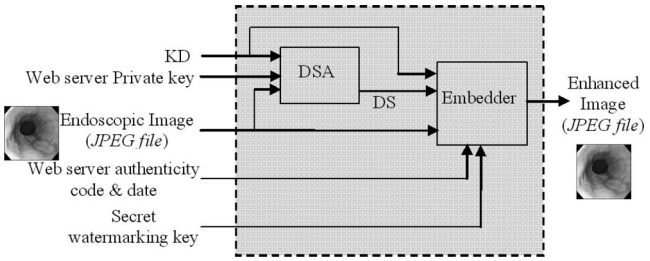

Fig. 9. Content of the "reliability protection and watermarking" box.

Web server, K_{pu} will be available and distributed by a trusted third party.

This DS, the KD, the Web server authenticity code, and the date of creation are concatenated in a single message that is then embedded in the JPEG-compressed image. The insertion can be made secret by using a watermarking secret key K_w, which will have to be known by the distant user to allow extraction of the hidden data. The user must, of course, be registered on the Web server.

Hence, when a user connects to the Web server, all data as well as watermarked images are publicly available. If he/she possesses the watermark extractor with the appropriate watermarking secret key, his/her system will extract the information.

Once the message is extracted, the unwatermarked image (i.e., the original compressed image), the KD, the DS, the Web server authenticity code, and the date of creation are recovered. Then, the user system checks information reliability by comparing the extracted DS to the recomputed one. For this task, a third party is requested to send the public key of the Web server where the image has been picked up from. This will also help each party to be authenticated as this key is user-dependent. Hence, if DSs are different, data integrity is lost and the system rejects the data. Otherwise, the system updates the user databases.

The watermark extractor, along with empty databases, KD management functions, and the user's language glossary will constitute the plug-in available to the registered user.

V. Conclusion

In this paper, we have proposed a new way to share and enhance medical image functionalities. While watermarking allows the sharing of information independently from the image format, the proposed knowledge digest gives a synthetic description of the image content, a digest that can be used for retrieving similar images with either the same findings or differential diagnoses. KD combined with watermarking appears to be a flexible solution to provide updates for distant user similarity rules, and case and knowledge databases.

In this paper, we have also extended a reversible scheme and applied it to JPEG-compressed images. It preserves image quality and may enable other useful applications similar to the e-learning demonstrator presented. Future work will focus on determining adaptively for any image the method parameters to ensure watermark invisibility (i.e., coefficient planes to select for embedding), optimizing the watermarking capacities of endoscopic images, in order to integrate more knowledge, i.e., the disease semiology level, and managing other file image formats like the recent JPEG 2000 format.

Acknowledgment

The authors would like to thank the Normed Verlag Editions (Homburg) for their authorization to use images extracted from their Atlas of Digestive Endoscopy.

References

[1] T. Lehmann, M. Güld, C. Thies, B. Fischer, K. Spitzer, D. Keysers, H. Ney, M. Kohnen, H. Schubert, and B. Wein, "Content-based image retrieval in medical applications," *Methods Inf. Med.*, vol. 43, no. 4, pp. 354–361, 2004.

[2] C. Le Guillou, J.-M. Cauvin, B. Solaiman, M. Robaszkiewicz, and C. Roux, "Information processing in upper digestive endoscopy," in *Proc. IEEE Int. Conf. ITAB*, 2000, vol. 76, pp. 183–188.

[3] J.-M. Cauvin, C. L. Guillou, B. Solaiman, M. Robaszkiewicz, P. L. Beux, and C. Roux, "Computer-assisted diagnosis system in digestive endoscopy," *IEEE Trans. Inf. Technol. Biomed.*, vol. 7, no. 4, pp. 256–262, Dec. 2003.

[4] R. Jain, S. Antani, and R. Kasturia, "A survey on the use of pattern recognition methods for abstraction, indexing and retrieval of images and video," *Pattern Recognit.*, vol. 35, no. 4, pp. 945–965, 2002.

[5] A. E. Plaza, "Case-based reasoning: Foundational issues, methodological variations, and system approaches," *Artif. Intell. Commun.*, vol. 7, no. 1, pp. 39–59, 1994.

[6] *Digital Imaging and Communications in Medicine (DICOM) Standard. (2007)* [Online]. Available: www.nema.org

[7] G. Coatrieux, H. Maitre, B. Sankur, Y. Rolland, and R. Collorec, "Relevance of watermarking in medical imaging," in *Proc. IEEE Int. Conf. ITAB*, Arlington, VA, 2000, pp. 250–255.

[8] G. Coatrieux, L. Lecornu, B. Sankur, and C. Roux, "A review of image watermarking applications in healthcare," in *Proc. Int. Conf. IEEE-EMBS—EMBC 2006*, Shanghai, China, Aug. 30–Sep. 3, pp. 4691–4694.

[9] C. Kim, "Compression of color medical images in gastrointestinal endoscopy: A review," *Med. Informatics*, vol. 9, pp. 1046–1050, 1998.

[10] G. Coatrieux, M. Lamard, W. Daccache, J. Puentes, and C. Roux, "A low distortion and reversible watermark application to angiographic images of the retina," in *Proc. IEEE IEEE-EMBC Conf.*, Shanghai, China, 2005, pp. 2224–2227.
[11] M. Crespi, M. Delvaux, M. Schapiro, C. Venables, and F. Zwiebel, "Minimal standard terminology for a computerized endoscopic database," *Amer. J. Gastroenterol.*, vol. 91, pp. 191–216, 1996.
[12] H. Akdag, M. De Glas, and D. Pacholczyck, "A qualitative theory of uncertainty," *Fundam. Inf.*, vol. 17, no. 4, pp. 333–362, 1992.
[13] C. Le Guillou, G. Coatrieux, J.-M. Cauvin, L. Lecornu, and C. Roux, "Enhancing shared medical image functionalities with image knowledge digest and watermarking," presented at the IEEE EMBS Conf. Inf. Technol. Appl. Biomed. (ITAB 2006), Ioannina, Greece, Oct.
[14] C. DeVleeschouwer, J.-F. Delaigle, and B. Macq, "Circular interpretation of bijective transformations in lossless watermarking for media asset management," *IEEE Trans. Multimedia*, vol. 5, no. 1, pp. 97–105, Mar. 2003.
[15] Official site of the Joint Photographic Experts Group (JPEG). (2007) [Online]. Available: www.jpeg.org
[16] M. Osada and H. Tsukui, "Development of ultrasound/endoscopy pacs (picture archiving and communication system) and investigation of compression method for cine images," in *Proc. SPIE Electron. Imag. Multimedia Technol. III*, Ioannina, Greece, 2002, vol. 4925, pp. 99–102.
[17] R. Rivest, A. Shamir, and L. Adleman, "A method for obtaining digital signature and public-key cryptosystems," *Commun. ACM*, vol. 21, no. 2, pp. 120–126, 1978.

Gouenou Coatrieux (M'06) received the Ph.D. degree in signal processing and telecommunication from the University of Rennes I, Rennes, France, in collaboration with the Ecole Nationale Supérieure des Télécommunications, Paris, France, in 2002.

His Ph.D. focused on watermarking in medical imaging. He is currently an Associate Professor in the Information and Image Processing Department, Institut TELECOM—TELECOM Bretagne, Brest, France, and his research is conducted in the LaTIM Laboratory, INSERM U650, Brest. His primary research interests concern medical information system security, watermarking, electronic patient records, and healthcare knowledge management.

Clara Le Guillou received the M.Sc. degree from the Université de Rennes I, Rennes, France, in 1998.

She is a Research Engineer. Her research is conducted in the LaTIM Laboratory, INSERM U650, Brest, France. Her primary research interest is the symbolic indexing and the medical reasoning. She has worked on upper digestive endoscopic images and collaborated in a new information system with a picture archiving and communication systems (PACS) in the hepato-gastro enterology hospital service. Since 2008, she has been at the Medical Information Department, Brest University Hospital, Brest, France, and participates in the MED1DEX project.

Jean-Michel Cauvin received the Medical Doctor degree from the Université de Bretagne Occidentale (UBO), France, in 1988 and specialized in digestive diseases, and the Ph.D. degree in symbolic indexation of endoscopic images and decision-aid systems from the Université de Rennes I, Rennes, France, in 2001.

Since 1996, he has been collaborating to the Medical Information Processing Laboratory (LaTIM—INSERM U650), Brest, France. He is currently a Physician in the Medical Information Department, Brest University Hospital, Brest. Since 2008, he has been steering the MED1DEX project, granted by the French Research Agency. His current research concerns medical indexing and computer-assisted systems.

Christian Roux (F'05) received the Aggregation degree in physics from the Ecole Normale Superieure, Cachan, France, in 1978, and the Ph.D. degree from the Institut National Polytechnique, Grenoble, France, in 1980.

In 1982, he joined the Institut TELECOM–TELECOM Bretagne, Brest, France, where he became an Associate Professor in 1987 and has been a Professor since 1987. He was a Visiting Professor with the Medical Image Processing Group, Department of Radiology, University of Pennsylvania (1992–1993), and a Distinguished International Research Fellow with the Department of Electrical Engineering, University of Calgary, Canada, in 1996 and 2003. He is the Director of the Laboratoire de Traitement de l'Information Médicale, INSERM U650—TELECOM Bretagne—UBO. His research interests concerns advanced medical information processing, and spatial, temporal, and functional information modeling and analysis in medical images, with applications in various medical domains including orthopedics, gastroenterology, ophthalmology, cardiology, and nuclear medicine. He has published around 110 papers, four book chapters, has edited three books, and holds three patents.

Dr. Roux was an Associate Editor of the IEEE TRANSACTIONS ON MEDICAL IMAGING (1993–2000), and is a member of the Editorial Board of the IEEE TRANSACTIONS ON INFORMATION TECHNOLOGY and the PROCEEDINGS OF THE IEEE. He serves as the President of the IEEE Engineering in Medicine and Biology Society in 2001.